FULL PAPER

Natural compounds in cancer prevention: effects of coffee extracts and their main polyphenolic component 5-CQA on oncogenic Ras proteins

Alessandro Palmioli,[#[a]] Carlotta Ciaramelli,[#[a]] Renata Tisi,[[a,b]] Michela Spinelli,[[a]] Gaia De Sanctis,[[a]] Elena Sacco,*[[a,c]] Cristina Airoldi*[[a,b,c]]

Abstract: Recent epidemiological studies demonstrate that consumption of healthy foods, especially rich in polyphenols content, might reduce the incidence of cancer and degenerative diseases. In particular, chlorogenic acids (CGAs) occur ubiquitously in food, representing the most abundant polyphenols in the human diet. A number of CGA beneficial biological effects, including anti-inflammatory activity, anti-carcinogenic activity and protection against neurodegenerative diseases have been reported. However, the molecular mechanisms at the basis of these biological activities have not yet been investigated in depth. By combining NMR spectroscopy, molecular docking, surface plasmon resonance and *ex vivo* assays on Ras-dependent breast cancer MDA-MB-231 cell line, we contributed to the elucidation of the molecular bases of the activity of CGAs and natural extracts from green and roasted coffee beans as chemo-protective dietary supplements.

Introduction

Fruits and vegetables are major sources of antioxidants, whose high levels in the diet seem to correlate with a reduction of some cancers and neurodegenerative diseases observed in people with high intakes of plant foods. In particular, several studies show polyphenol effects on the MAP kinase (ERK, JNK, p38) pathway and PI3 kinase/Akt signaling cascades.[1] One important family of antioxidant polyphenols is represented by chlorogenic acids (CGAs), soluble esters formed between phenolic hydroxycinnamates and quinic acid. Depending on the acyl moiety identity, number and position, CGAs can be divided into various groups, being the most common *p*-coumaroylquinic acids, caffeoylquinic acids (CQAs), feruloylquinic acids (FQAs) and dicaffeoylquinic acids (diCQAs).[2]

Particularly high levels of chlorogenic acid (5-*O*-caffeoylquinic acid, 5-CQA) (Figure 1) have been found in coffee beans used to prepare green coffee and, after roasting, black coffee, a widespread drink worldwide.[3] Together with coffee, a primary dietary source of chlorogenic acids is tea. It occurs ubiquitously in food, in fact high contents of 5-CQA have been found in sunflower seeds, berry fruits, chicory and globe artichoke and, if at lower levels, it has also present in Chinese parsley, potatoes, tomatoes, apples, pears, lettuce and eggplant.[4]

In 2005 Feng and coworkers[5] reported that 5-CQA protects against environmental carcinogen-induced carcinogenesis and suggested that its chemopreventive effects are related to the suppression of ROS-mediated NF-κB, AP-1 and MAPK activation. Although through different signals transduction pathways, all these proteins locate downstream to the small GTPase Ras (Figure 2), whose somatic mutations are the most common activating lesions found in human cancer.[6] Thus, the observation that 5-CQA presents structural similarities with low molecular weight Ras inhibitors synthesized in our laboratory[7] (exemplified by compound **1** depicted in Figure 1) led us to investigate its ability to target Ras proteins, aimed at deepening the molecular mechanisms at the basis of its protective activity.

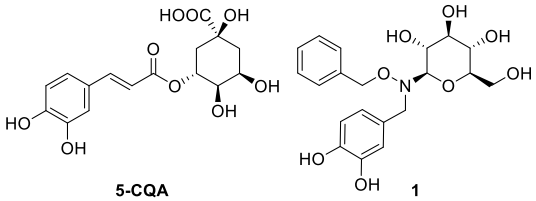

Figure 1. Structures of 5-CQA and compound **1**.

Although oncogenic mutations in Ras proteins are considered a major target in anticancer drug discovery, they are generally associated with poor response to standard therapies.[8] In addition, despite efforts to develop inhibitors of these oncoproteins have covered more than three decades, no effective pharmacological inhibitor of the Ras oncoprotein has reached the clinic until now.[9] In the light of these evidences, the idea to identify a natural compound, very abundant in human diet, able to down-regulate Ras signaling, thus becoming eventually suitable for therapy and prevention of Ras-dependent cancer, sounds very exciting.

[a] Dr A. Palmioli, Dr C. Ciaramelli, Dr M. Spinelli, G. De Sanctis, Dr R. Tisi, Dr E. Sacco and Dr C. Airoldi
Department of Biotechnology and Biosciences
Università degli Studi di Milano-Bicocca
Piazza della Scienza 2, 20126 Milan, Italy.
E-mail: elena.sacco@unimib.it; cristina.airoldi@unimib.it
[b] Dr. R. Tisi, Dr C. Airoldi
NeuroMI Milan Center for Neuroscience, University of Milano-Bicocca, 20126 Milano, Italy
[c] Dr E. Sacco and Dr C. Airoldi
SysBio Center of Systems Biology
Piazza della Scienza 2, 20126 Milan, Italy

# These authors contributed equally to this work.

Supporting information for this article is given via a link at the end of the document.

To this purpose, we combined NMR spectroscopy, molecular docking, SPR and *ex vivo* assays on cancer cell lines, to verify 5-CQA ability to bind Ras proteins, interfering with the Ras-dependent signal transduction and thus reducing cancer cell proliferation.

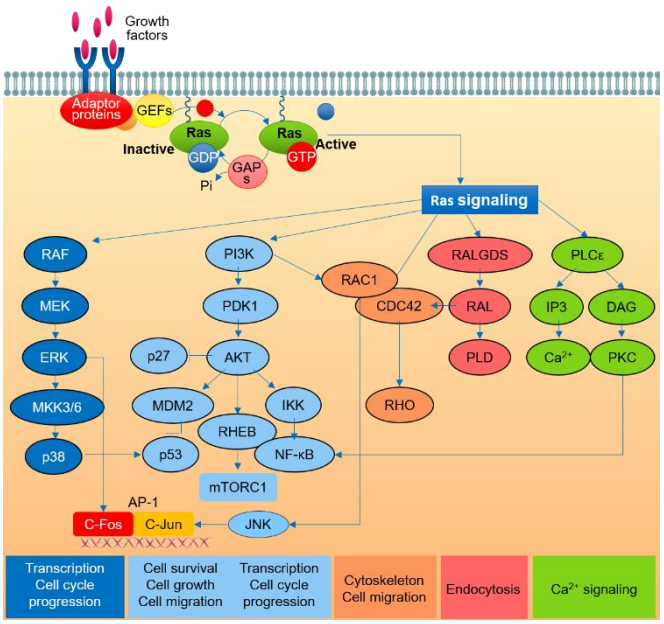

Figure 2. Ras protein signalling in mammalian cells. In humans, *RAS* genes encode four distinct but highly homologous 21-kDa Ras proteins: H-Ras, N-Ras, K-Ras4A and K-Ras4B (the last two proteins being alternative splice variants of the *K-RAS* gene). Ras proteins act as transducers that couple cell surface receptors to intracellular effectors and alternate between on and off conformation that are conferred by binding to GTP or GDP, respectively. Under physiological conditions, the transitions between these two states is finely regulated by guanine nucleotide exchange factors (GEFs), which promote the activation of Ras by stimulating GDP for GTP exchange, and by GTPase activating proteins (GAPs), which accelerate Ras-mediated GTP hydrolysis. Altering this fine balance by deregulation of either GAP or GEF activity may result in hypo- or hyper-activation of downstream pathway(s), so that overexpression of a GEF or inactivation of a GAP may both result in cell transformation. Main Ras-dependent downstream effectors are schematized in the figure, which are involved in many aspects of the tumor phenotype such as promotion of proliferation, suppression of apoptosis, metabolic reprogramming, remodeling of the microenvironment, evasion of the immune response and metastasis.[10]

Results and Discussion

5-CQA binds wt H-Ras and its oncogenic variant H-Ras G13D. First of all, the binding of 5-CQA to Ras proteins was investigated by STD NMR spectroscopy.[11] This approach, based on a robust, versatile and sensitive experiment, has been successfully exploited in the past, allowing the screening of small libraries of synthetic Ras ligands.[7, 12]

STD NMR experiments were carried out on ligand/protein mixtures dissolved in deuterated phosphate buffer (PB) (pH 7.4, 25 °C). To a solution of wt H-RasGDP dissolved in PB, 5-CQA was added to reach a final concentration of 50 μM for the protein and 2 mM for the compound. Experiments were acquired by saturating the protein resonances at 0.00 ppm to achieve the selective saturation of some aliphatic protein resonances. The presence of 5-CQA NMR signals in the STD spectrum (Figure 3B) is a non-ambiguous demonstration of the interaction with the protein. Analogous results were obtained when the same experiment was performed on a mixture containing a H-Ras oncogenic variant, namely G13D. This mutation, found in many types of human cancers, results in a rapid nucleotide exchange and consequently constitutive activated Ras signaling.[12d, 13]

For both the proteins, STD experiments were acquired with six different saturation times (0.5, 1.0, 1.5, 2.0, 2.5 and 3.0 s), allowing to obtain the STD amplification factor for each 5-CQA proton giving STD signals (Supporting Information - Figure S1). Values obtained in the presence of the two proteins are of the same magnitude, suggesting a very similar affinity for the two proteins (Supporting Information -Table S1).

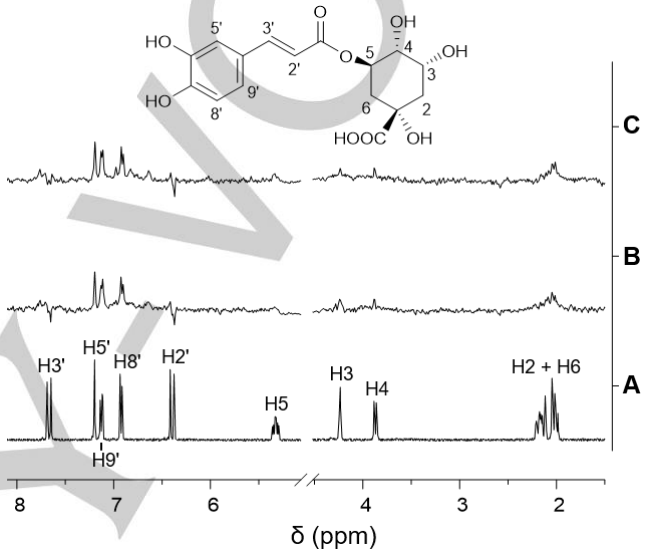

Figure 3. ^{1}H-NMR spectrum of 2 mM 5-CQA in deuterated phosphate buffer (**A**); STD NMR spectra recorded on a mixture containing 2 mM 5-CQA and 50 μM wt H-RasGDP (**B**) or 50 μM H-RasGDP G13D (**C**). Spectra were acquired with 1280 scans and 2s of saturation time, at 25 °C and 400 MHz.

The STD-based epitope-mapping for the ligand is reported in Figure 4.

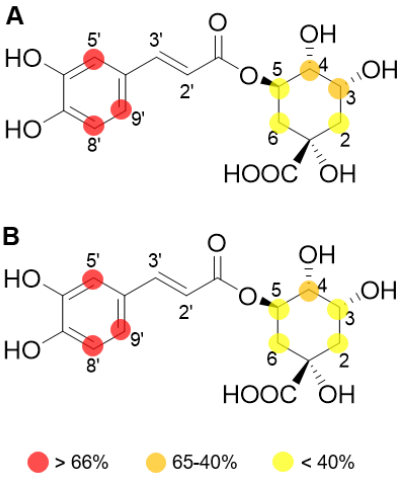

Figure 4. 5-CQA binding epitope to wt H-Ras (**A**) and H-Ras G13D (**B**) obtained for 2 s of saturation time. In both the cases, the largest absolute amplification factor (A_{STD}) was scaled to 100%.

According to the STD-relative intensities, the region of the ligand mainly involved in the interaction with both wt and mutant H-Ras is the aromatic ring, while protons of the quinic acid moiety show less intense STD signals. Notably, no STD effect was observed for protons 2' and 3'.

Molecular Docking suggests 5-CQA putative binding site on Ras protein.

For molecular docking, H-Ras protein in both active (GTP-bound) or inactive (GDP-bound) conformations were considered, since a major conformational change, occurring after GDP substitution with GTP is involved in the interaction with Ras effectors (Figure 5).

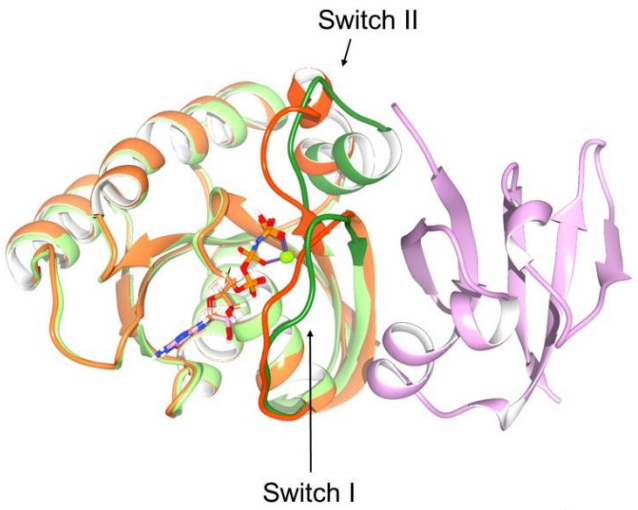

Figure 5. H-Ras structure determinants involved in the interactions with its effector Raf1 RBD (Ras Binding Domain, light purple) comprises the Switch I and Switch II motifs, that display a conformational change from the GDP-bound (green) to the GTP-bound (orange) form of H-Ras. The GTP nucleotide and the Mg^{2+} ion involved in ligand binding (green) are shown.

To identify 5-CQA putative binding sites on these protein targets, an initial survey based on blind docking was performed with SwissDock protein ligand docking web service powered by EADock DSS (from the Molecular Modeling group of the Swiss Institute of Bioinformatics). The survey identified several clusters of docking poses in four different binding sites for H-RasGTP, which displayed similar top FullFitness scores, and several clusters of docking poses in four binding sites for H-RasGDP with similar top scores, but the ranking of the clusters in the different binding sites were not the same for the active/inactive protein conformations (Supporting Information - Figure S2).

Top scoring poses were identified for both protein complexes in the nucleotide binding site (see Figure 5), named the Switch I pocket (S-I-P), and this site was further characterized although competition with the nucleotide itself likely excludes that this could be an available site for 5-CQA binding. The survey also identified a putative binding site in a pocket under the Switch II loop (named S-II-P), which was previously reported as targeted by Ras inhibitors.[14] Furthermore, a binding pocket was identified in both the protein complexes, labeled as BP (Back Pocket), and involving the 105-110 and 138-140 loops besides the C-terminal end of α5 helix. This pocket, although displaying a SwissDock score similar to the other sites, was not further investigated since it is far from the effector and guanine-nucleotide-exchange factor binding sites, and thus it is not expected to give any significant effect on Ras activity. The same was considered for the α4β6 binding site, retrieved in H-RasGTP SwissDock survey.

The selected binding pockets (i.e., S-I-P and S-II-P for both complexes, besides S-I-II-P for H-RasGDP complex only) were utilized for receptor grid generation to perform a Glide XP protocol docking. S-I-P allowed the ligand poses with best scores, but the other two pockets were also retained since the docking scores for the best ligand poses were significantly low.

The best scoring complex for each binding pocket was submitted as a receptor grid defining complex to the Induced Fit docking protocol, in order to allow the protein to undergo sidechain or backbone movements during the docking in a zone within 7 Å to the ligand. This has allowed the loops surrounding the binding pocket to adapt to the ligand presence, significantly improving the scoring of the poses. The ligand poses obtained were scored by Glide docking Gscore, Glide Emodel and IFD (Induced Fit Docking) scores (Table 1).

Table 1. Scoring parameters for the top ranking ligand poses obtained by Induced Fit protocol for 5-CQA docking to either H-RasGDP or H-RasGTP complex in the indicated binding sites. For S-I-P, the nucleotide was removed from the complex before docking.

Receptor[a]	Binding Site[b]	Docking Gscore	Glide Emodel	IFD score
H-RasGDP	S-I-P	-10.026	-112.11	-5677.061
H-RasGDP	S-II-P	-8.881	-106.462	-6094.946
H-RasGDP	S-I-II-P, A	-8.598	-96.165	-5525.692
H-RasGDP	S-I-II-P, B	-7.801	-70.532	-5492.228
H-RasGTP	S-I-P	-12.368	-141.729	-7087.101
H-RasGTP	S-II-P	-8.561	-92.106	-7281.481

[a] H-RasGDP (PDB:4q21), H-RasGTP (PDB:5p21). [b] Binding sites are defined in the text and illustrated in Figure S2.

Glide Emodel was considered since it is the best scoring parameter to discriminate among different complexes between a protein and the same ligand, but docking Gscore was also reported, as in the S-I-P binding site, the nucleotide had to be removed, affecting Glide Emodel scoring of the binary complexes when compared to the ternary complexes. IFD score tentatively estimates the energy of the protein-ligand complex, so it can only be compared among complexes with identical components (i.e., not for poses with H-Ras bound to different nucleotides). The best scoring poses in each binding site were reported in Figure 6.

The poses in the S-I-P binding pocket, although displaying very good scoring and likely characterized by the best binding affinity, were not represented since the H-Ras-nucleotide complex is very stable (with dissociation constants in the picomolar order, unless a specific guanine exchange factor is present) and the chance of 5-CQA competing for the nucleotide binding site is far remote, when considering micromolar range of GTP concentration within living cells.[15]

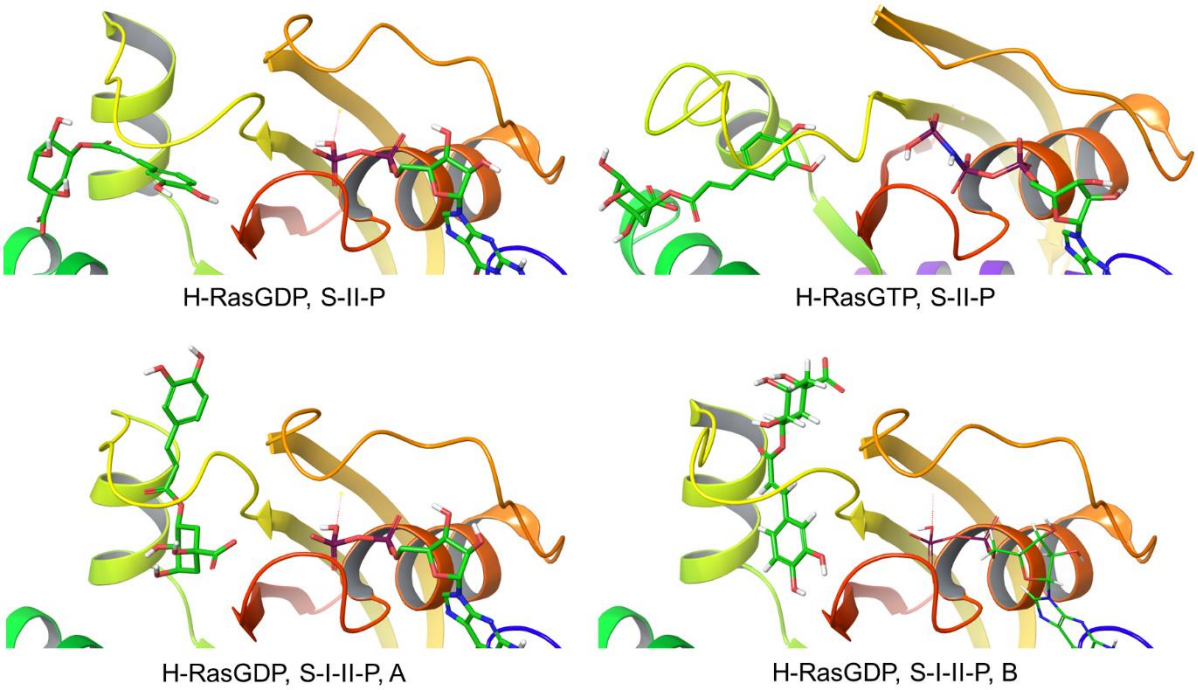

Figure 6. Induced Fit docking protocol best scoring results for the indicated H-Ras complex in the indicated pockets. Switch I is in orange (and it defines the nucleotide binding site, where nucleotide is shown) and Switch II in yellow.

Two different ligand poses were displayed for H-RasGDP binding site S-I-II-P, since the binding epitope identified in Figure 4 suggest pose B shows a best agreement with NMR epitope binding data, despite showing the worst scoring parameters**5-**

CQA interferes with Ras interaction with activators and effectors.

Docking analyses suggested poses for 5-CQA on Ras regions potentially critical for binding with both Ras activators and effectors.[14] Therefore, we decided to perform surface plasmon resonance (SPR) analyses in order to verify if 5-CQA was able to affect the interaction between Ras proteins and the catalytic domain of RasGRF1 (RasGRF1$_{cat}$) (Figure 7A) or the Ras-binding domain (RBD) of Raf-1 (Raf1$_{RBD}$), (Figure 7B), chosen as models of Ras activators and effectors respectively.

To this purpose, we monitored the real time association and dissociation of GST-tagged RasGRF1$_{cat}$ and Raf1$_{RBD}$ to/from His-tagged RasGDP and His-tagged RasGTP, immobilized onto a NTA-sensor chip, in the absence and in the presence of 500 µM 5-CQA. These experiments showed that 5-CQA reduces both RasGRF1$_{cat}$ binding to Ras-GDP and Raf-1$_{RBD}$ binding to Ras-GTP, demonstrating that this molecule can inhibit Ras interaction with both its activators and effectors. In particular, the presence of 5-CQA does not affect the kinetic properties of either RasGRF1$_{cat}$ binding to Ras-GDP (k_{on} ~$4x10^4$ $M^{-1}s^{-1}$, and k_{off} ~$1.5x10^{-4}$ s^{-1}) or Raf-1$_{RBD}$ binding to Ras-GTP (k_{on} ~$1.5x10^4$ $M^{-1}s^{-1}$ and k_{off} ~$2-3x10^{-4}$ s^{-1}), but only the maximal capacity of binding, suggesting a non-competitve inhibition, which is compatible with the computationally predicted site of 5-CQA binding to Ras, distinct from the interaction sites of both the GEF and the effector. These data suggest that 5-CQA could act by interfering with the GEF-mediated nucleotide exchange required for Ras activation and/or by shutting down the effector-mediated signal transduction downstream the protein.

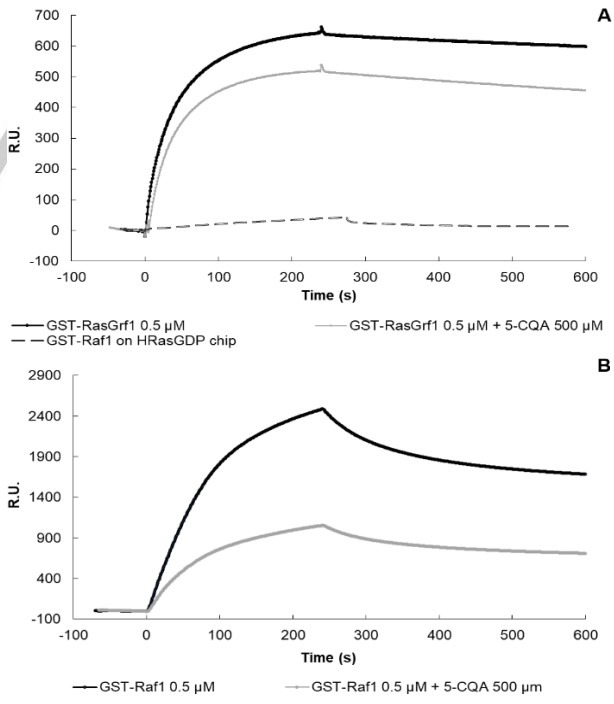

Figure 7. Representative sensograms obtained from SPR experiments performed using NTA sensor chips with pre-immobilized His-H-RasGDP (**A**) or His-H-RasGTP (**B**). (**A**) Analysis performed using as analyte 0.5µM GST-RasGRF1cat in presence or absence of 500µM 5-CQA or 0.5µM GST-Raf1$_{RDB}$ as indicated. (**B**) Analysis performed using as analyte 0.5µM GST-Raf1$_{RDB}$ in presence or absence of 500µM 5-CQA.

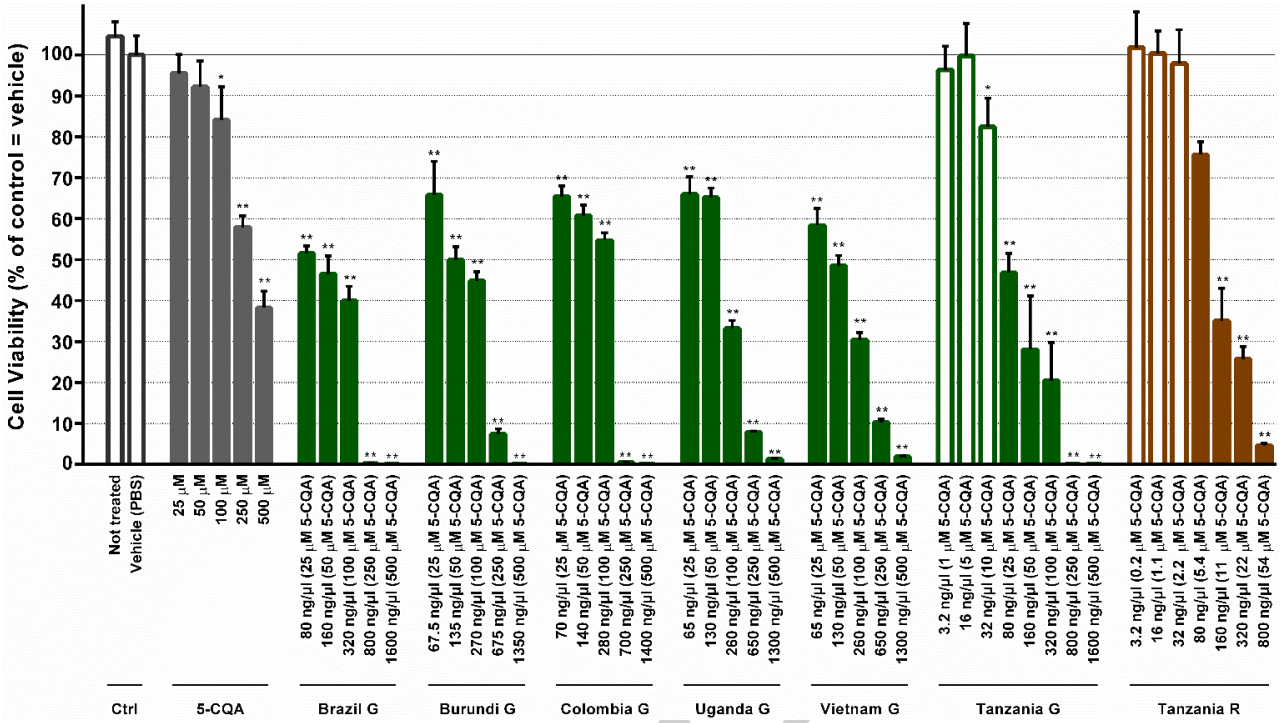

Figure 8. Viability of MDA-MB-231 cells treated for 72h with 0, 25, 50, 100, 250 and 500 µM pure 5-CQA, or with amounts (from 0 to 1,6µg/µl as indicated) of green (G) coffee extracts, with different geographical origin, containing the corresponding concentration of 5-CQA was analyzed using RealTime-GloTM MT Cell Viability Assay. Arabica (Brazil, Burundi and Colombia) and Robusta (Uganda, Vietnam and Tanzania) coffees were assayed. Of the most effective green coffee, Tanzania, a wider range of concentration including those containing 1, 5 and 10 µM 5-CQA (empty green bars) was analyzed. Roasted extract of Tanzania (Tanzania R) was analyzed at the same total concentrations of the green extract (Tanzania G). Data are expressed as the percentage of cell viability (%) relative to vehicle (PBS) treated control cells. The data represent the average of 2 or 3 independent experiments, each performed in triplicate, ± standard deviation. Two-tailed Student's t-test results were reported: * p<0.01, ** p<0.001 treated vs control (vehicle).

The majority of Ras inhibitors able to bind directly the protein developed so far targeted the GDP/GTP nucleotide exchange, in order to prevent protein activation.[16] Nevertheless, due to the extremely high affinity of Ras proteins for GTP/GDP,[17] this task resulted very hard. In fact, Ras oncogenic mutations that impair GTP hydrolysis result in constitutive activation of the protein.[18] In these conditions, the nature of the nucleotide bound to Ras becomes more dependent on the relative nucleotide affinity and concentration, facilitating GTP binding over GDP,[19] and increasing the population of active GTP-bound Ras molecules. For these reasons, in many cases the inhibition of Ras activation resulted poorly effective. However, compounds able to interfere with Ras interaction with its effectors can switch-off Ras-dependent signal transduction, irrespectively of the protein activation state. In the light of these considerations, 5-CQA ability to exert this role sounds very interesting, in particular when its abundance in human diet is taken into account.

5-CQA modulate Ras-dependent cancer cell line proliferation. As previously mentioned, the aberrant hyper-activation of Ras proteins is often associated with tumor onset and progression. Thus, after demonstrating that 5-CQA interferes *in vitro* with Ras interaction with its effectors, its ability to modulate Ras-mediated signal transduction that promotes cell proliferation was investigated. To this purpose, invasive breast cancer cell line MDA-MB-231, expressing the oncogenic RasG13D variant, was employed. Cells were plated at low-density (3000 cell/cm^2) and, after 24 h, treated for 72 h with increasing concentrations of 5-CQA. The number of viable cells was measured using the RealTime plate assay-Glo™ MT Cell Viability Assay (Promega, # G9713). As controls, equivalent amounts of vehicle, i.e. PBS buffer in which the compound had been dissolved, was employed. Figure 8 resumes the obtained results, clearly indicating that 5-CQA exerts an inhibitory effect on MBA-MB-231 cellular proliferation in a dose-dependent manner, with a calculated IC_{50} of about 300 µM (Table 2).

Table 2. 5-CQA or coffee extracts IC_{50} calculated on the basis of MDA-MB-231 cells viability assay and relative to vehicle (PBS-treated cells). For the coffee extracts also the concentration of 5-CQA equivalent contained was reported. IC_{50} values were determined by non linear growth sigmoidal Hill curves fitting the viability results reported in Figure 8.

	IC_{50}	IC_{50} of 5-CQA eq contained in extracts
5-CQA	330 ± 16 µM	-
Brazil G	102 ± 10 ng/µl	32 ± 3 µM
Burundi G	137 ± 22 ng/µl	51 ± 8 µM
Colombia G	315 ± 17 ng/µl	113 ± 6 µM
Uganda G	180 ± 9 ng/µl	69 ± 3 µM
Vietnam G	119 ± 17 ng/µl	46 ± 7 µM
Tanzania G	72 ± 7 ng/µl	23 ± 2 µM
Tanzania R	121 ± 10 ng/µl	82 ± 0.7 µM

Green and roasted coffee extracts interfere with Ras-dependent cancer cell line proliferation.

Being green coffee one of the edible matrix with the highest content of CGAs, in particular 5-CQA,[3] we decided to investigated the potential bioactivity of green coffee extracts (GCEs) too.

GCEs were prepared from grinded green coffee beans by ultrasound-assisted hydroalcoholic extraction.[20] In particular, six different geographical origins, i.e. Brazil, Burundi, Colombia, Tanzania, Vietnam and Uganda, were selected. Three coffees belonged to the specie Arabica (Brazil, Burundi and Colombia) and three to the specie Robusta (Tanzania, Vietnam and Uganda). The metabolic profiling of each GCE was characterized through ^{1}H-NMR. A representative spectrum, obtained for GCEs from Tanzania beans, is reported in Figure 9A.

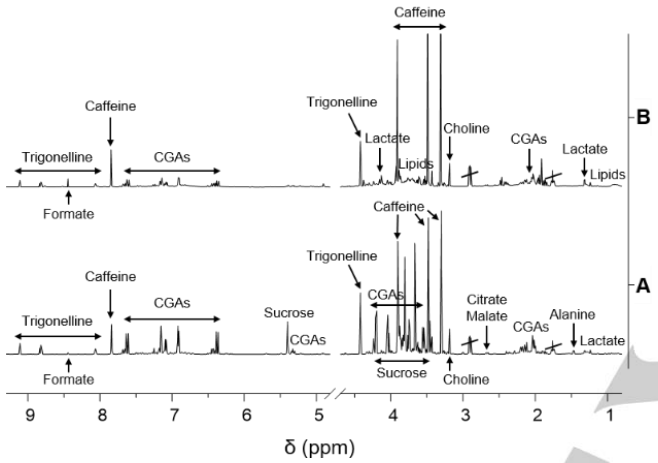

Figure 9. ^{1}H-NMR spectra of green (**A**) and roasted (**B**) coffee extracts obtained for Tanzania origin. Each sample contained 5 mg/ml of extract, dissolved in 10 mM deuterated phosphate buffer, pH 7.4, DSS 1 mM. Spectra were acquired at 25 °C and 600 MHz. Resonances of the most important metabolites are assigned.

In agreement with data previously reported,[20-21] the most abundant metabolites in hydroalcoholic GCEs are sucrose, caffeine, trigonelline and CGAs. Among CGAs, 5-CQA shows the highest concentration regardless of the geographical origin, as shown in Figure 10.

To verify if the presence of other GCE metabolites could interfere with 5-CQA binding to Ras proteins, STD experiments were repeated on mixtures containing wt H-RasGDP or H-RasGDP G13D and one of the six GCEs. STD acquired in the presence of H-Ras G13D and GCE obtained from Tanzania coffee beans is represented in Figure 11 as example. The appearance of 5-CQA resonances in the STD spectrum (Figure 11B) is an unequivocal demonstration of the binding to the protein. The same result was achieved when ligand-receptor interaction studies were performed in the presence of the other GCEs (data not shown).

These results demonstrated that 5-CQA binding to Ras is not hindered by the other constituents of GCEs.

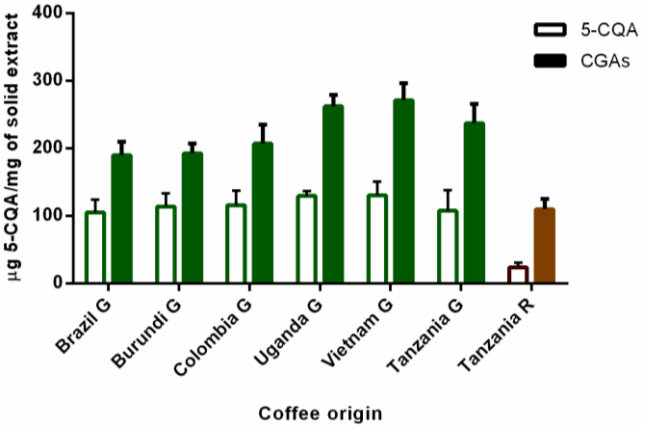

Figure 10. 5-CQA and total CGAs content in GCEs (**G**) and RCE (**R**), as determined by quantitative ^{1}H-NMR spectra. Concentrations are expressed as μg of 5-CQA per mg of solid coffee extract. Results are reported as the mean ± SD of 3 independent experiments.

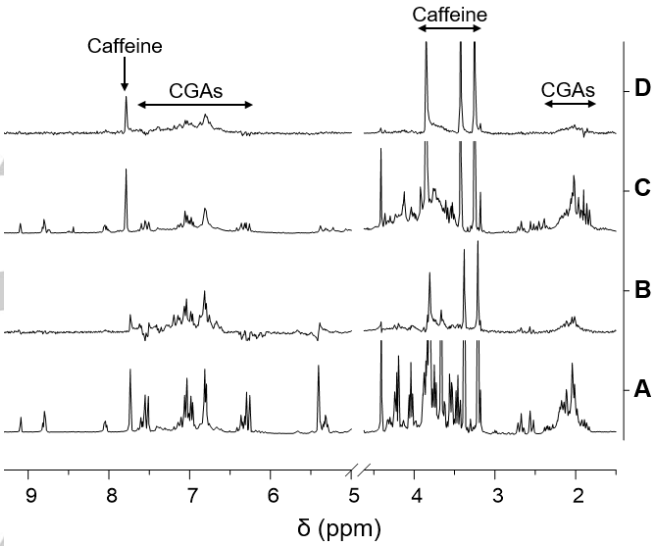

Figure 11. ^{1}H-NMR spectra of samples containing 15 mg/ml of GCE (**A**) or RCE (**C**) obtained from Tanzania coffee beans. STD NMR spectra recorded on a mixture containing 50 μM H-RasGDP G13D and the same GCE (**B**) or RCE (**D**) reported in **A** and **C** respectively. STD spectra were acquired with 1280 scans and 2 s of saturation time at 25 °C and 400 MHz.

A carefully inspection of STD spectra reveals the presence not only of 5-CQA, but also of caffeine resonances, suggesting an interaction of this molecule with the target protein. Nevertheless, caffeine signals are also visible in blank STD spectra recorded in the absence of Ras, indicating its putative interaction with other macromolecules present into the extracts (Supporting Information - Figure S3).

GCEs ability to affect MDA-MB-231 cell proliferation was then investigated. The same experiments previously described to test pure 5-CQA activity was performed by treating MDA-MB-231 cells with increasing concentrations of the six GCEs extracts (Figure 8). GCE amounts were selected to contain the same concentrations of 5-CQA tested previously. Notably, not only GCEs resulted active in reducing cell growth, but, for equal contents of 5-CQA, their calculated IC_{50} values were about one order of magnitude lower compared with 5-CQA one (Table 2). In particular, the lowest value was 23 μM, obtained for Tanzania origin (Table 2). These findings suggest that, in addition to 5-CQA, GCEs contain

other bioactive molecules able to modulate cancer cell proliferation. These molecules may also exert an additive or synergistic effect with 5-CQA activity; the same 5-CQA, besides acting as a ligand and modulator of Ras proteins, as supposed on the bases of our *in vitro* assays, is a potent antioxidant able to prevent oxidative stress. We can also rule out that some of the GCE components may increase bioavailability and / or favor 5-CQA cell uptake.

As well as in green coffee, 5-CQA is present in roasted coffee too, even if at a lower concentration (Figure 10), as a consequence of the roasting process.[22] However, being its consumption greater compared to that of green coffee, we decided to also test the biological activity of a coffee extract obtained from medium-roasted coffee beans. Since, according to the screening performed on GCEs, extract prepared from beans originating from Tanzania resulted the most active, the biological activity of corresponding roasted extract was investigated.

Roasted coffee extract (RCE) from Tanzania beans was obtained with the same procedure described for GCEs. The corresponding ^{1}H-NMR spectrum is reported in Figure 9B. From the comparison between GCE (Figure 9A) and RCE (Figure 9B) NMR profilings, it results clear that in RCE sucrose resonances disappeared almost completely and CGAs experienced a significant reduction, consistent with the formation of melanoidines during the roasting.[21c] In particular, the CGAs total content decreases from 23.7% present in Tanzania GCE to 11% w/w of solid extract measured in RCE, and 5-CQA concentration varies from 10.8% to 2.4% w/w of solid extract moving from Tanzania GCE to RCE (Figure 10).

STD experiments performed in the presence of wt H-Ras or H-Ras G13D (Figure 11D) confirmed that 5-CQA contained in RCE retains its ability to recognize and bind the proteins.

Also RCE inhibited MDA-MB-231 cell proliferation in a dose-dependent manner, but at higher concentration (IC_{50}=121±10 ng/µl) if compared with the corresponding GCE (IC_{50}=72±7 ng/µl, Figure 8). This correlates with the reduction in 5-CQA and CGAs content, suggesting an actual contribution of these compounds to the coffee extract biological activities assayed in MDA-MB-231 cancer cells.

5-CQA and coffee extracts modulate the activation/phosphorylation state of p42/p44 MAPKs

To correlate the inhibition of MDA-MB-231 cell proliferation with the modulation of Ras signaling pathway, the effect of 5-CQA and GCE and RCE prepared form Tanzania coffee beans on the activation/phosphorylation state of p42/p44 MAPKs was evaluated in the same cell line. p42/p44 MAPKs are Ras effectors (Figure 2), whose phosphorylation at Thr202/Tyr204 residues occurs after Ras pathway activation.[23]

In particular, the effect of 1 h-treatment with a concentration of 5-CQA, GCE or RCE equivalent to their respective IC_{50} values calculated in the viability assay was measured in basal conditions (medium containing 10% serum) and under 15'-stimulation with EGF after 2 h serum starvation. In fact, although serum provides optimal conditions for cell growth, serum starvation-based protocol is more indicated to study the normal (physiological) response to growth factors, including the Ras-dependent MAPKs activation. MDA-MB-231 cells were plated at high density (6000 cells/cm^2) in 6-well plates in medium containing 10% serum. After 24 h, the cells seeded in half of the wells were serum-starved for 2 h and the 1 h-treatment with 5-CQA, GCE or RCE was performed on all the wells, possibly followed by 15'-stimulation with EGF in the case of serum-starved cells. Then, cell lysates were generated from each well, which were used to evaluate the activation/phosphorylation state of p42/p44 MAPKs with PathScan® Phospho-p44/42 MAPK (Thr202/Tyr204) Sandwich ELISA Kit (Cell Signaling Technology). As expected, we observed a correlation between the inhibition of MDA-MB-231 cell proliferation and the lower activation/phosphorylation state of p42/44 MAPKs, which was reduced of about 40-60% both in basal conditions and under EGF stimulation after serum starvation upon 5-CQA/GCE/RCE treatment (Figure 12).

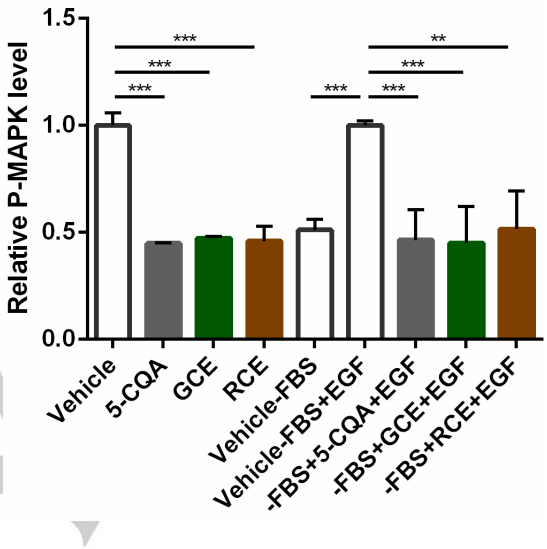

Figure 12. Phospho-p44/42 MAPK level in cell lysates derived from MDA-MB-231 cells treated as indicated in the graph was determined by using the ELISA assay PathScan® Phospho-p44/42 MAPK (Thr202/Tyr204) Sandwich ELISA Kit (Cell Signaling Technology). In detail MDA-MB-231 cells were 2h-serum starved and/or 1h-treated with a concentration of 5-CGA, green or roasted Tanzania coffee extracts corresponding to their specific IC_{50}. At the end of serum starvation cells were stimulated with EGF 100 ng/mL for 15 min. Data shown are mean +/- standard deviation of two independent experiments.

Being MAPK activity reduced also upon RCE treatment, we demonstrated that the roasting process does not negatively affect the biological activity of the coffee extract.

Conclusions

The experimental data collected provide a clear indication that 5-CQA, one of the most abundant polyphenol present in human diet, is able to modulate the activity of Ras proteins, considered as a major target in anticancer drug discovery.

Combining results from STD NMR, SPR and molecular docking experiments, we can speculate that its mechanism of action is based on the inhibition, upon binding to the target, of Ras interaction with both activators and effectors. In addition, viability and p42/p44 MAPKs activation/phosphorylation assays performed on MDA-MB-231 cells suggested its capability of reducing cancer cells growth.

Notably, when edible natural extracts containing significant concentrations of 5-CQA, i.e. green and roasted coffees, were

tested according to the same experimental protocol, a higher biological activity was found, suggesting an additive or synergistic effect of their different components. The calculated IC_{50} values are not compatible with those expected for a potent antitumor drug (fortunately, being GCE and RCE natural extracts regularly taken with the diet), but low enough to prompt the possible use of diet supplements based on decaffeinated coffee extracts for preventive purposes.

In addition, the structural requirements for 5-CQA binding to Ras proteins here reported, in particular the ligand binding epitope derived from STD experiments, can be exploited for the rational drug-design of new Ras inhibitors able to disrupt their binding to activators and effectors, since all previous attempts for targeting GDP/GTP nucleotide exchange have been unsuccessful.

Furthermore, due to the growing interest in nutraceutical and functional food sciences, our approach based on the combination of different and robust *in vitro* and *ex vivo* assays can be exploited for the screening of natural edible matrixes aimed at the identification of bioactive compounds.

Experimental Section

General

Unless otherwise stated, all materials used in this work were from Sigma-Aldrich (St. Louis, MO, USA). Reagent-grade water used to prepare all solutions was obtained from a Milli-Q (Millipore, Bedford, MA, USA) purification system.

NMR Spectroscopy binding studies

NMR data were recorded on a Varian 400 MHz Mercury instrument for experiments on H-RasGDP wt and H-RasGDP G13D and 5-CQA or coffee extracts. Coffee extracts (final concentration 15 mg/ml) or 5-CQA (final concentration 2 mM) and Ras-GDP complex (final concentration 50 µM) were dissolved in 10 mM deuterated phosphate buffer. The pH of each sample was adjusted to pH 7.4 with NaOD and/or DCl. Total sample volumes were 560 µl. Basic sequences were employed for STD experiments. For STD, a train of Gaussian shaped pulses of 50 ms was used to selectively saturate the protein envelope; the total saturation time of the protein envelope was adjusted by the number of shaped pulses and was varied between 0.5 and 3.0 s. The on- and off-resonance spectra were acquired in an interleaved mode with the same number of scans (1280 scans on-res and 1280 scans off-res). The on-resonance frequency was set to 0.00 ppm. All spectra were recorder with a 40 ms spin lock pulse, which minimizes the background protein resonances. No protein resonances can be detected, since they have relaxed within this period. Reference experiments with samples containing only 5-CQA or coffee extracts were performed under the same experimental conditions to verify true ligand binding. Spectra were processed with a line broadening of 0.3 Hz, phased and baseline corrected and the signal suppression was applied.

Green and roasted coffee extraction

Grinded green and medium-roasted coffee beans were received from Beyers Koffie, Belgium. Coffee extracts were obtained using a hydro-alcoholic extraction procedure. Briefly, 200 mg of grinded sample was extracted with 20 ml of a mixture of acidified (with 0.1M HCl) water (pH 4.5; 70%) and methanol (30%) by sonication at 37 kHz for 15 min in an ultrasound bath (Elmasonic P 30 H, Elma Schmidbauer GmbH, Singen, Germany) at 30 °C. After 1 h, the solutions were filtered through cotton wool and 0.45 µm PTFE filters (Pall Corporation, Port Washington, NY, USA), concentrated under reduced pressure at 40 °C and freeze-dried. The lyophilized samples were stored at -20 °C.

NMR metabolic profiling of coffee extracts

Freeze-dried samples were suspended in 10 mM deuterated phosphate buffer (PB, pH 7.4) at a final concentration of 5 mg/ml, sonicated (37 kHz, 20 min) and centrifuged (9425 *xg*, 10 min, 20 °C, ScanSpeed 1730R Labogene, Lynge, Sweden). 4,4-dimethyl-4-silapentane-1-sulfonic acid (DSS, final concentration 0.5 mM) was added to the obtained supernatant as an internal reference for both concentrations and chemical shift. The pH of each sample was verified with a Microelectrode (Mettler Toledo, Columbus, OH, USA) for a 5 mm NMR tubes and adjusted to a value of 7.4 with NaOD or DCl. All pH values were corrected for the isotope effect. The acquisition temperature was 25 °C. All spectra were acquired on an AVANCE III 600 MHz NMR spectrometer (Bruker, Billerica, MA, USA) equipped with a QCI (^{1}H, ^{13}C, ^{15}N/^{31}P and 2H lock) cryogenic probe and a Varian Mercury 400 MHz spectrometer. ^{1}H-NMR spectra were recorded with water suppression (cpmgpr1d pulse sequences in Bruker library) and 64 scans, spectral width of 20 ppm, relaxation delay of 30 s. They were processed with a line broadening of 0.3 Hz, automatically phased and baseline corrected. Chemical shift values were internally calibrated to the DSS peak at 0.0 ppm. Compound identification and assignment were performed with the support of 2D NMR experiments, comparison to reported assignments[21a, 21b] and the SMA analysis tool integrated in MestreNova software.[24] In particular, ^{1}H,^{1}H-TOCSY (Total Correlation SpectroscopY) spectra were acquired with 48 scans and 512 increments, a mixing time of 80 ms and relaxation delay was 2 seconds. ^{1}H,^{13}C-HSQC (Heteronuclear Single Quantum Coherence) spectra were acquired with 48 scans and 256 increments, a relaxation delay of 2 s. For metabolite quantification, the global spectrum deconvolution (GSD) algorithm, available in the MNova software package (MestReNova v 10.0, 2016, Mestrelab Research, Santiago de Compostela, Spain) was exploited. In this way, overlapping regions were deconvoluted, and absolute quantification was performed also for metabolites with resonances in rare crowded spectral areas. For each compound, the mean value of the different assigned signals was determined.

Molecular Docking

To identify potential binding sites of 5-CQA, an automated molecular-docking procedure was performed, either on an active, GTP-bound human H-Ras (PDB: 5p21) or on an inactive, GDP-bound human H-Ras (PDB: 4q21), by the web-based SwissDock platform (http://www.swissdock.ch/).[25] The docking was performed using the default parameters, with no region of interest defined (blind docking). The top score binding sites identified were further submitted to finer docking analysis in Maestro 10.1 (Schrödinger) (https://www.schrodinger.com/citations#Maestro). All docking calculations were performed using the Glide software (Glide, version 6.7, Schrödinger, LLC, New York, NY, 2015). The receptor based molecular docking was carried forward after preparing ligands, proteins, and preparation of grid formation of the putative binding site of protein. GLIDE docking eXtra Precision (XP) protocol was used, validating the binding cavities identified by the online survey considering. GLIDE molecular docking output GScore (empirical scoring function), which is calculated by calculating ligand–protein interaction energies, root mean square deviation (RMSD), hydrogen bonds, hydrophobic interactions, internal energy, π–π stacking interactions and desolvation. Finally, the best positions identified by Glide XP protocol were used as the input for grid receptor definition in induced-fit docking (IFD) workflow with flexible ligand option, in order to generate alternative conformations of the receptor suitable to bind 5-CQA, by allowing the protein to undergo sidechain or backbone movements during the docking (Schrödinger Suite 2015-2 Induced Fit Docking protocol; Glide version 6.7, Schrödinger, LLC, New York, NY, 2015; Prime version 4.0, Schrödinger, LLC, New York, NY, 2015). The IFD extended sampling protocol was employed, generating up to 20 poses per ligand on each iteration. The OPLS 2005 force field[26] was used for the minimisation stage, in which residues within 7 Å of each ligand pose were optimised. All other parameters were set to their default values.

Protein expression and purification

Recombinant N-terminal His-tagged H-Ras (wt or G13D) proteins were purified from *E.coli* M15 [pREP4] strain expressing a pQE^{TM}-derived

plasmid (Qiagen, Valencia, CA), as previously described in Palmioli et al. [12d] In detail protein expression was induced with 1mM IPTG at a cell density corresponding to an absorbance of 0.6 at 600 nm. Cells were grown at 30 °C for 4h after induction and then harvested by centrifugation. Crude extracts were obtained by sonication of cells suspended in lysis buffer (50 mM NaH_2PO_4 pH 7.5, 300 mM NaCl, 10 mM imidazole, 5 mM 2-mercaptoethanol, 0.5% triton-X 100, plus protease inhibitors). 3 ml of lysis buffer for each gram of cells were used. Clarified supernatants were loaded onto a Ni-NTA Agarose affinity column (Qiagen) equilibrated with lysis buffer. The resin was washed with 10 volumes of wash buffer (50 mM NaH_2PO_4, 300 mM NaCl, 20 mM imidazole, pH 7.5). His-tagged proteins were then eluted with elution buffer (50 mM NaH_2PO_4, 300 mM NaCl, 250 mM imidazole, pH 7.5 10µM GDP). Fractions containing the eluted proteins were pooled and dialyzed overnight against buffer (50 mM Tris-HCl pH 7.5, 50 mM NaCl, 50% glicerol, 5 mM 2-mercaptoethanol, 10µM GDP) using Dialysis Tubing cellulose 10mm (14,000Da cut-off D9277 Sigma Aldrich) and conserved to –20°C. Purified Ras proteins were preloaded with GTP according to the protocol previously described.[27] The glutathione S-Transferase (GST)-tagged Ras-GEF domain of murine RasGRF1 (residues 976-1262 of the mature protein; $RasGRF1_{cat}$) and GST-tagged RBD domain of human cRaf1 (residues 1-149 of the mature protein; $Raf1_{RBD}$ were purified from *E. coli* BL21pLysE expressing a pGEX2T-derived plasmid using standard glutathione-Sepharose chromatography (Amersham Biosciences). In detail, protein expression was induced with 0,1mM IPTG at a cell density corresponding to an absorbance of 0.4-0.6 at 600nm. Cells were grown at 30 °C for 4h after induction and then harvested by centrifugation. Crude extracts were obtained by sonication of cells suspended in lysis buffer (140 mM NaCl, 2.7 mM KCl, 10.1 mM Na_2HPO_4, 1.8 mM KH_2PO_4, 1 mM EDTA, 5 mM 2-mercaptoethanol, 1mM PMSF, 0.5% triton-X 100, pH 7.3 supplemented with cocktail inhibitors (Roche)). Clarified supernatants were loaded onto a Glutathione Sepharose 4B affinity column (GE Healthcare) equilibrated with PBS. The resin was washed with 10 volumes of PBS. The bound GST fusion proteins were subsequently eluted with buffer (20 mM glutathione, 100 mM Tris-HCl pH 8, 120 mM NaCl, 0.1% Triton X-100). Fractions containing the eluted proteins were pooled and dialyzed overnight against buffer (50 mM Tris-HCl, 50 mM NaCl, 50% glicerol, 5 mM 2-mercaptoethanol, pH 7.5) and conserved to –20°C.

SRP analysis

Surface Plasmon Resonance (SPR) experiments[28] were carried out with a BIAcoreX system (BIAcore, GEHealthcare). His-tagged HRas bound to GDP or GTP (as indicated) was coupled to sensor chips-NTA (carboxymethylated dextran matrix pre-immobilized with Nitrilo Triacetic Acid (NTA); BIAcore, GEHealthcare). A surface density of c.a. 4500/5000 resonance units was generated for His-HRas-GDP, and His-HRas-GTP respectively. No nickel solution was injected over the reference cell. Analytes of binding assays were $GST\text{-}RasGRF1_{cat}$ and $GST\text{-}Raf1_{RBD}$. All experiments were performed in HBS-P+ buffer (BIAcore, GE Healthcare) maintaining a flow rate of 10µl/min. Surface regeneration was accomplished by injecting 350mM EDTA in running buffer (30 sec contact) two or three times. Evaluation of binding kinetics was performed using the Biaevaluation software, version 3.0 (Biacore Inc.), by considering 1 : 1 Langmuir interaction. Notably, k_{off} measured in SPR experiments cannot correspond to the physiological dissociation constants since the absence of free nucleotide in the experiments significantly affects this parameter.

Cell proliferation assay

MDA-MB-231 cells were plated at low density (3000 cell/cm^2) in 96-well plates and incubated at 37°C and 5% CO_2 overnight. After 24 hours, cells were treated with 5-CQA or with GCE or RCE at different concentrations. After 72 h from the treatment, MT Cell Viability Substrate 500 X and NanoLuc® 500 X reagents from RealTime-Glo™ MT Cell Viability Assay (Promega, # G9713) were added to culture media and luminescence at different time points from the treatment was read with Victor Multilabel Plate Reader (Perkin Elmer). Viability of cells treated with increasing concentrations of 5-CQA or GCE or RCE was tested relatively to viability of the same cells treated with vehicle (PB buffer). Viability results were analyzed with OriginPro 8.0 software using a non linear 'growth-sigmoidal Hill' curve (n = 1), to calculate the relative IC_{50} values.

Assay of activation/phosphorylation state of p42/p44

MDA-MB-231 cells were plated at high density (6000 cells/cm^2) in 6-well plates in medium containing 10% serum and incubated at 37 °C and 5% CO_2 overnight. After 24 h, the effect of 1 h treatment with a concentration of 5-CQA, GCE or RCE equivalent to their IC_{50} values calculated in the viability assay (330µM, 72 ng/µl and 121 ng/µl respectively) was measured in basal conditions (medium containing 10% serum) and under 15'-stimulation with EGF after 2 h of serum starvation. Particularly, the cells seeded in half of the wells were serum-starved for 2 h and the 1 h-treatment with 5-CQA, GCE or RCE was performed on all the wells, possibly followed by 15'-stimulation with EGF in the case of serum-starved cells. Then, cell lysates were generated from each well by using Shalloway buffer[29] added with protease inhibitor cocktail (Roche), Cell lysates were then used to evaluate the activation/phosphorylation state of p42/p44 MAPKs with PathScan® Phospho-p44/42 MAPK (Thr202/Tyr204) Sandwich ELISA Kit (#7177 Cell Signaling Technology) following manufacturer's instructions. Finally, MAPK activity was normalized on protein content, measured with Bradford assay[30].

Acknowledgements

Coffee bean samples were provided from Beyers Koffie, Belgium. C.A. thanks AIRC for funding project n° MFAG-17030 and Fondazione CARIPLO and Regione Lombardia for funding project n° 2015-0763.

Keywords: cancer prevention • chlorogenic acid • coffee extracts • NMR molecular recognition studies • Ras proteins

References

[1] D. Vauzour, A. Rodriguez-Mateos, G. Corona, M. J. Oruna-Concha, J. P. Spencer, *Nutrients* **2010**, *2*, 1106-1131.

[2] M. N. Clifford, *Journal of the Science of Food and Agriculture* **2000**, *80*, 1033-1043.

[3] a) M. Lepelley, G. Cheminade, N. Tremillon, A. Simkin, V. Caillet, J. McCarthy, *Plant Sci* **2007**, *172*, 978-996; b) G. S. Duarte, A. A. Pereira, A. Farah, *Food Chem* **2010**, *118*, 851-855.

[4] J. A. Rothwell, J. Perez-Jimenez, V. Neveu, A. Medina-Remón, N. M'Hiri, P. García-Lobato, C. Manach, C. Knox, R. Eisner, D. S. Wishart, A. Scalbert, *Database* **2013**, *2013*, bat070-bat070.

[5] R. Feng, Y. Lu, L. L. Bowman, Y. Qian, V. Castranova, M. Ding, *Journal of Biological Chemistry* **2005**, *280*, 27888-27895.

[6] I. A. Prior, P. D. Lewis, C. Mattos, *Cancer research* **2012**, *72*, 2457-2467.

[7] a) A. Palmioli, E. Sacco, S. Abraham, C. J. Thomas, A. D. Domizio, L. D. Gioia, V. Gaponenko, M. Vanoni, F. Peri, *Bioorganic & Medicinal Chemistry Letters* **2009**, *19*, 4217-4222; b) E. Sacco, S. J. Abraham, A. Palmioli, G. Damore, A. Bargna, E. Mazzoleni, V. Gaponenko, M. Vanoni, F. Peri, *MedChemComm* **2011**, *2*, 396-401.

[8] E. Sacco, M. Spinelli, M. Vanoni, *Expert opinion on therapeutic patents* **2012**, *22*, 1263-1287.

[9] H. Ledford, *Nature* **2015**, *520*, 278-280.

[10] D. K. Simanshu, D. V. Nissley, F. McCormick, *Cell* **2017**, *170*, 17-33.

[11] a) M. Mayer, B. Meyer, *Angewandte Chemie* **1999**, *111*, 1902-1906; b) M. Mayer, B. Meyer, *Angew Chem Int Edit* **1999**, *38*, 1784-1788; c) C. Airoldi, S. Merlo, E. Sironi, in *Applications of NMR Spectroscopy, vol. 2*, Bentham Science Publishers Ltd, **2015**, pp. 147-219; d) C. Airoldi, S. Sommaruga, S. Merlo, P. Sperandeo, L. Cipolla, A. Polissi, F. Nicotra, *Chemistry* **2010**, *16*, 1897-1902; e) C. Airoldi, S. Sommaruga, S. Merlo, P. Sperandeo, L. Cipolla, A. Polissi, F. Nicotra, *ChemBioChem* **2011**, *12*, 719-727; f) C. Airoldi, S. Giovannardi, B. La Ferla, J. Jimenez-Barbero, F. Nicotra, *Chemistry* **2011**, *17*, 13395-13399.

[12] a) F. Peri, C. Airoldi, S. Colombo, S. Mari, J. Jimenez-Barbero, E. Martegani, F. Nicotra, *Eur J Org Chem* **2006**, 3707-3720; b) C. Airoldi, A. Palmioli, A. D'Urzo, S. Colombo, M. Vanoni, E. Martegani, F. Peri, *Chembiochem* **2007**, *8*, 1376-1379; c) C. Muller, M. A. G. Z. Frau, D. Ballinari, S. Colombo, A. Bitto, E. Martegani, C. Airoldi, A. S. van Neuren, M. Stein, J. Weiser, C. Battistini, F. Peri, *Chemmedchem* **2009**, *4*, 524-528; d) A. Palmioli, E. Sacco, C. Airoldi, F. Di Nicolantonio, A. D'Urzo, S. Shirasawa, T. Sasazuki, A.

Di Domizio, L. De Gioia, E. Martegani, A. Bardelli, F. Peri, M. Vanoni, *Biochemical and Biophysical Research Communications* **2009**, *386*, 593-597; e) S. Colombo, A. Palmioli, C. Airoldi, R. Tisi, S. Fantinato, S. Olivieri, L. De Gioia, E. Martegani, F. Peri, *Current cancer drug targets* **2010**, *10*, 192-199.

[13] M. J. Smith, B. G. Neel, M. Ikura, *P Natl Acad Sci USA* **2013**, *110*, 4574-4579.

[14] J. M. Ostrem, U. Peters, M. L. Sos, J. A. Wells, K. M. Shokat, *Nature* **2013**, *503*, 548-+.

[15] T. W. Traut, *Mol Cell Biochem* **1994**, *140*, 1-22.

[16] A. D. Cox, S. W. Fesik, A. C. Kimmelman, J. Luo, C. J. Der, *Nat Rev Drug Discov* **2014**, *13*, 828-851.

[17] J. John, R. Sohmen, J. Feuerstein, R. Linke, A. Wittinghofer, R. S. Goody, *Biochemistry-Us* **1990**, *29*, 6058-6065.

[18] a) J. B. Gibbs, I. S. Sigal, M. Poe, E. M. Scolnick, *P Natl Acad Sci-Biol* **1984**, *81*, 5704-5708; b) M. Trahey, F. McCormick, *Science* **1987**, *238*, 542-545.

[19] A. Scherer, J. John, R. Linke, R. S. Goody, A. Wittinghofer, E. F. Pai, K. C. Homes, *Journal of molecular biology* **1989**, *206*, 257-259.

[20] L. Amigoni, M. Stuknytė, C. Ciaramelli, C. Magoni, I. Bruni, I. De Noni, C. Airoldi, M. E. Regonesi, A. Palmioli, *Journal of Functional Foods* **2017**, *33*, 297-306.

[21] a) F. Wei, K. Furihata, F. Hu, T. Miyakawa, M. Tanokura, *J Agric Food Chem* **2011**, *59*, 9065-9073; b) F. F. Wei, K. Furihata, M. Koda, F. Y. Hu, T. Miyakawa, M. Tanokura, *J Agr Food Chem* **2012**, *60*, 1005-1012; cD. Perrone, A. Farah, C. M. Donangelo, *J Agr Food Chem* **2012**, *60*, 4265-4275.

[22] J. K. Moon, H. S. Yoo, T. Shibamoto, *J Agr Food Chem* **2009**, *57*, 5365-5369.

[23] S. Meloche, J. Pouyssegur, *Oncogene* **2007**, *26*, 3227-3239.

[24] C. Cobas, F. Seoane, S. Domínguez, S. Sykora, A. Davies, *Spectrosc. Eur* **2011**, *23*, 26-30.

[25] a) A. Grosdidier, V. Zoete, O. Michielin, *Nucleic acids research* **2011**, *39*, W270-277; b) A. Grosdidier, V. Zoete, O. Michielin, *J Comput Chem* **2011**, *32*, 2149-2159.

[26] J. L. Banks, H. S. Beard, Y. X. Cao, A. E. Cho, W. Damm, R. Farid, A. K. Felts, T. A. Halgren, D. T. Mainz, J. R. Maple, R. Murphy, D. M. Philipp, M. P. Repasky, L. Y. Zhang, B. J. Berne, R. A. Friesner, E. Gallicchio, R. M. Levy, *J Comput Chem* **2005**, *26*, 1752-1780.

[27] C. Lenzen, R. H. Cool, A. Wittinghofer, *Methods in enzymology* **1995**, *255*, 95-109.

[28] a) M. Malmqvist, *Biochemical Society transactions* **1999**, *27*, 335-340; b) R. L. Rich, D. G. Myszka, *Curr Opin Biotech* **2000**, *11*, 54-61.

[29] S. J. Taylor, D. Shalloway, *Current biology : CB* **1996**, *6*, 1621-1627.

[30] M. M. Bradford, *Analytical biochemistry* **1976**, *72*, 248-254.

Entry for the Table of Contents

FULL PAPER

By combining NMR spectroscopy, molecular docking, surface plasmon resonance and *ex vivo* assays on Ras-dependent breast cancer MDA-MB-231 cell line, we contributed to the elucidation of the molecular bases of the activity of chlorogenic acids and natural extracts from green and roasted coffee beans as chemo-protective dietary supplements.

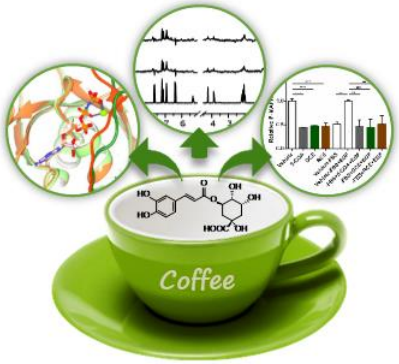

Alessandro Palmioli, Carlotta Ciaramelli, Renata Tisi, Michela Spinelli, Gaia De Sanctis, Elena Sacco, Cristina Airoldi**

Page No. – Page No.

Natural compounds in cancer prevention: effects of coffee extracts and their main polyphenolic component 5-CQA on oncogenic Ras proteins